Article

NMR Analysis of Surfaces and Interfaces in 2-nm CdSe

Mia G. Berrettini, Gary Braun, Jerry G. Hu, and Geoffrey F. Strouse

J. Am. Chem. Soc., **2004**, 126 (22), 7063-7070• DOI: 10.1021/ja037228h • Publication Date (Web): 12 May 2004

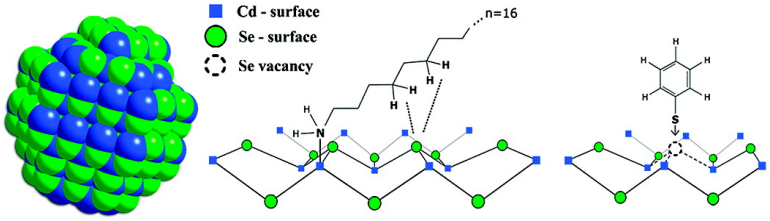

More About This Article

Additional resources and features associated with this article are available within the HTML version:

- Supporting Information
- Links to the 14 articles that cite this article, as of the time of this article download
- Access to high resolution figures
- Links to articles and content related to this article
- Copyright permission to reproduce figures and/or text from this article

View the Full Text HTML

J|A|C|S
ARTICLES
Published on Web 05/12/2004

NMR Analysis of Surfaces and Interfaces in 2-nm CdSe

Mia G. Berrettini,[†,‡] Gary Braun,[§] Jerry G. Hu,*[,§] and Geoffrey F. Strouse*[,†,‡,§]

Contribution from the Department of Chemistry and Biochemistry, Florida State University, Tallahassee, Florida 32306-4390, and Mitsubishi Chemical Center for Advanced Materials and Materials Research Laboratory, University of California, Santa Barbara, California 93106

Received July 11, 2003; E-mail: Strouse@chem.fsu.edu

Abstract: Solid-state NMR analysis on wurtzite 2-nm hexadecylamine-capped CdSe nanocrystals (CdSe-HDA) provides evidence of discrete nanoparticle reconstruction within the Se sublattice of the nanomaterial. The cadmium and selenium atoms are probed with $^{1}H-^{113}Cd$ and $^{1}H-^{77}Se$ cross-polarization magic angle spinning (MAS) experiments, which demonstrate five ordered selenium sites in the nanoparticle that can be assigned to contributions arising from different surface sites and a selenium site one layer down from the surface. Intriguingly, in these materials both HDA and thiophenol are observed to selectively bind to specific sites on the nanoparticle surface. 2D heteronuclear chemical shift correlation (HETCOR) experiments provide evidence for thiophenol selectively binding at surface vacancies. Analysis of the NMR provides a model of a 2-nm CdSe-HDA molecular surface.

Semiconductor nanocrystals have attracted considerable attention since they offer a unique opportunity to observe the evolution of their physical properties with size. This has led to applications in a wide range of areas.[1−10] Understanding the correlation between the thermodynamic stability and fundamental structural properties of nanomaterials, which is influenced by the nanocrystal (NC) type, size, and passivating layer, is an important area. Of particular interest is the understanding of the surface chemistry, surface reconstruction, and the associated perturbations of the electronic properties of the materials arising from surfaces in nanoscale materials.[11−17] As the nanomaterial is reduced in size, the contribution from surface to core species changes, leading to a condition where surface reconstruction should be observable by solid-state NMR methods, such as spin−echo and cross-polarization magic angle spinning (CPMAS) techniques. CdSe nanocrystals, which are widely studied in the nanoscience community, provide a great model system to investigate the surface structure and interfaces for semiconductor nanocrystals, because of the presence of NMR active ^{113}Cd and ^{77}Se.

The structure of a nanomaterial can be envisioned as consisting of a core inorganic structure reminiscent of a bulk structure, surrounded by a reconstructed inorganic surface shell, and capped by an organic passivating layer, reminiscent of a self-assembled monolayer.[18−22] The impact on the structural attributes of nanocrystals can be delineated into four distinct regions of the NCs (Figure 1). The passivation layer, region A, can be envisioned as a three-dimensionally constrained monolayer of tightly packed organic amphiphiles that act to thermodynamically stabilize the surface through a headgroup−surface interaction.[21,22] Region B consists of the molecular level interaction between the surface atoms and the headgroup of the passivant and the outermost Cd and Se sites, which is at the inorganic−organic interface.[34,35] Region C encompasses the top

† Florida State University.
‡ Mitsubishi Chemical Center for Advanced Materials, University of California.
§ Materials Research Laboratory, University of California.

(1) Bhargava, R. N.; Chhabra, V.; Som, T.; Ekimov, A.; Taskar, N. *Phys. Status Solidi B* **2002**, *229*, 897−901.
(2) De la Torre, J.; Souifi, A.; Lemiti, M.; Poncet, A.; Busseret, C.; Guillot, G.; Bremond, G.; Gonzalez, O.; Garrido, B.; Morante, J. R. *Physica E* **2003**, *17*, 604−606.
(3) Modreanu, M.; Gartner, M.; Aperathitis, E.; Tomozeiu, N.; Androulidaki, M.; Cristea, D.; Hurley, P.; Maltings, L. *Physica E* **2003**, *16*, 461−466.
(4) Irrera, A.; Pacifici, D.; Miritello, M.; Franzo, G.; Priolo, F.; Iacona, F.; Sanfilippo, D.; Di Stefano, G.; Fallica, P. G. *Physica E* **2003**, *16*, 395−399.
(5) Pacifici, D.; Irrera, A.; Franzo, G.; Miritello, M.; Iacona, F.; Priolo, F. *Physica E* **2003**, *16*, 331−340.
(6) Milliron, D. J.; Alivisatos, A. P.; Pitois, C.; Edder, C.; Frechet, Jean, M. J. *Adv. Mater.* **2003**, *15*, 58−61.
(7) Yang, H.; Holloway, P. H.; Ratna, B. B. *J. Appl. Phys.* **2003**, *93*, 586−592.
(8) Wang, D.; Rogach, A. L.; Caruso, F. *Nano Lett.* **2002**, *2*, 857−861.
(9) Michalet, X.; Pinaud, F.; Lacoste, T. D.; Dahan, M.; Bruchez, M. P.; Alivisatos, A. P.; Weiss, S. *Single Mol.* **2001**, *2*, 261−276.
(10) Tran, P. T.; Goldman, E. R.; Anderson, G. P.; Mauro, J. M.; Mattoussi, H. *Phys. Status Solidi B* **2002**, *229*, 427−432.
(11) Tolbert, S. H.; Alivisatos, A. P. *Science* **1994**, *265*, 373.
(12) Bowen Katari, J. E.; Colvin, V. L.; Alivisatos, A. P. *J. Phys. Chem.* **1994**, *98*, 4109−4117.
(13) Dai, Y.; Han, S.; Dadi D.; Zhang, Y.; Qi, Y. *Solid State Commun.* **2003**, *126*, 103−106.
(14) Pellegrino, P.; Garrido, B.; Garcia, C.; Ferre, R.; Moreno, J. A.; Morante, J. R. *Physica E* **2003**, *16*, 424−428.
(15) Ispasoiu, R. G.; Lee, J.; Papadimitrakopoulos, F.; Goodson, T. *Chem. Phys. Lett.* **2001**, *340*, 7−12.
(16) Koberling, F.; Mews, A.; Basche, T. *Adv. Mater.* **2001**, *13*, 672−676.
(17) Cordero, S. R.; Carson, P. J.; Estabrook, R. A.; Strouse, G. F.; Buratto, S. K. *J. Phys. Chem. B* **2000**, *104*, 12137−12142.
(18) Becerra, L. R.; Murray, C. B.; Griffin, R. G.; Bawendi, M. G. *J. Chem. Phys.* **1994**, *100*, 3297−3300.
(19) Luedtke, W. D.; Landman, U. *J. Phys Chem.* **1996**, *100*, 13323−13329.
(20) Hostetler, M. J.; Wingate, J. E.; Zhong, C.-J.; Harris, J. E.; Vachet, R. W.; Clark, M. R.; Londono, J. D.; Green, S. J.; Stokes, J. J.; Wignall, G. D.; Glish, G. L.; Porter, M. D.; Evans, N. D.; Murray, R. W. *Langmuir* **1998**, *14*, 17−30.
(21) Meulenberg, R. W.; Bryan, S.; Yun, C. S.; Strouse, G. F. *J. Phys. Chem B* **2002**, *106*, 7774−7780.
(22) Meulenberg, R. W.; Strouse, G. F. *J. Phys. Chem. B* **2001**, *105*, 7438−7445.
(23) Aldana, J.; Wang Y. A.; Peng, X. *J. Am. Chem. Soc.* **2001**, 123, 8844−8850.

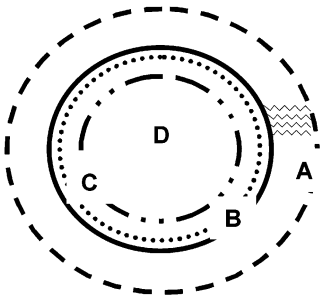

Figure 1. (A) Organic passivating layer. (B) Cd or Se atoms at surface. (C) Second layer from surface. (D) Nanoparticle core in wurtzite symmetry.

layer of the nanomaterials and one crystallographic plane down that are prone to reconstruction,[23−26] and region D consists of the NC core, which is predicted to be minimally affected by surface interactions. Although particle reconstruction may occur in the core, the organic passivant-driven surface reconstruction has recently been suggested to be influential to the observed optical properties of CdSe nanomaterials.[23−25] In fact, surface reconstruction in nanomaterials has been observed in spherical 17 and 28 Å InAs nanocrystals by extended X-ray absorption fine structure (EXAFS).[26] In recent nuclear magnetic resonance (NMR) studies, similar surface reconstruction findings have been reported in Ti nanoparticles.[27] Unfortunately, the surface interfacial region represents the most difficult to analyze experimentally, because of the low ratio of surface species relative to core species in nanoscale materials.

Several studies to date have used analysis of (spin−lattice) T_1 and (spin−spin) T_2 relaxations in both solid-state and solution phase NMR as a probe of the nanomaterial surface and core structure.[18,28−31,33−35] Sachleben et al. have shown that the T_2 in thiols appended to CdS is sensitive to the chemical environment of binding.[34] More recent studies using ^{113}Cd have suggested the surface cadmium atoms can be clearly distinguished from the core cadmium atoms.[28,29] These in depth studies in NMR on CdSe and other nanomaterials provide an ideal platform to test predictions of structural reconstruction of the different regions in a CdSe nanomaterial. By conducting ^{13}C, ^{1}H, ^{113}Cd, and ^{77}Se NMR (for example in CdSe), direct insight into regions A, B, and C can be gained, providing further correlating experimental data for the development of a model of the passivant layer interactions on the nanocrystal surface. Application of cross-polarization magic angle spinning in the solid-state allows the surface to be selectively studied,[28,29] while other techniques such as spin−echo sequences allow the entire nanomaterial to be addressed.[30,31] As observed in previous studies on layered silicate surfactant mesophases, NMR can provide insight into the degree of crystallinity and reconstruction of the material, as well as knowledge of the connectivities of surface atoms through two-dimensional techniques.[32]

In this article, 2-nm hexadecylamine-capped CdSe nanocrystals (CdSe-HDA) prepared by a single source precursor route[36] are studied through solution and solid-state NMR to probe the nature and structure of the ligands binding to the surface of the particle, as well as to distinguish the sites of cadmium and selenium. Through analysis of solution and solid-state ^{13}C NMR, solid-state ^{77}Se and ^{113}Cd spin−echo, and CPMAS NMR experiments, as well as ^{13}C{^{1}H}, ^{113}Cd{^{1}H}, and ^{77}Se{^{1}H} 2D heteronuclear chemical shift correlation (HETCOR) NMR experiments, a model of the surface and interfaces of this material was developed.

Experimental Section

Synthesis of 2-nm CdSe Nanocrystals (CdSe-HDA). CdSe nanocrystals were prepared by a previously published single source precursor method.[36] Approximately 2.1 g of $Li_4[Cd_{10}Se_4(SC_6H_5)_{16}]$ (0.653 mmol) was heated in 75 g of HDA to 120 °C under argon. The reaction progress was followed by UV−vis absorbance spectroscopy and removal from heat when the desired nanocrystal size of 2-nm was reached. UV−vis experiments were carried out on the hot reaction mixture by direct sampling of the reaction mixture (1−5 μL) and dilution of the aliquot into 3 mL of chloroform. The onset of the absorption profile was characteristic of the size in nanomaterials. After cooling to 50 °C, the CdSe sample was precipitated by the addition of approximately 200 mL of methanol and was collected by centrifugation. Purification and size selection was accomplished by dissolution in a minimum amount of chloroform, reprecipitation by addition of methanol, and centrifugation (3×).

Ligand Exchange with 2,4-Difluorothiophenol. Approximately 2 mL of 2,4-difluorothiophenol was added to 100 mg of CdSe-HDA. The mixture was stirred for 5−10 min at 60 °C under argon. After being cooled to room temperature, approximately 5 mL of methanol was added, and the material was collected by centrifugation. The sample was then dissolved in a minimum amount of chloroform and precipitated via the addition of methanol. This washing sequence was repeated three times, followed by a final rinse with methanol and being dried overnight under vacuum.

NMR. Solution NMR experiments were performed at room temperature on a Bruker 500 MHz Avance spectrometer with a HX double resonance broadband probe operating at 125.8 and 500.1 MHz for ^{13}C and ^{1}H, respectively. The ^{13}C experiment was performed with a single pulse on ^{13}C while decoupling ^{1}H during acquisition. Typical parameters were: acquisition time 0.33 s, recycling delay 10 s, and a 90° pulse length of 15.3 μs.

Solid-state MAS NMR experiments were performed at room temperature on a Bruker 300 MHz Avance spectrometer with a 4-mm broadband MAS probe double tuned to ^{1}H (300.1 MHz) and the X channel to ^{13}C (75.5 MHz), ^{77}Se (57.2 MHz), or ^{113}Cd (66.6 MHz). A spinning speed of 12 kHz was used in all experiments. The MAS ^{13}C NMR experiments on 2-nm CdSe-HDA and ligand-exchanged CdSe-HDA were performed under the conditions of two pulse phase modulated (TPPM) ^{1}H decoupling, an acquisition time of 24 ms, and a recycling delay of 20 s.

The chemical shifts of ^{1}H, ^{13}C, ^{77}Se, and ^{113}Cd were referenced to TMS, TMS, $(NH_4)_2SeO_4$ (1040 ppm relative to $Se(CH_3)_2$ at 0 ppm), and to 0.5 M $Cd(NO_3)_2$ solution (0 ppm), respectively.

(24) Meulenberg, R. W.; Strouse, G. F. *Phys. Rev. B* **2002**, *66*, 035317.
(25) Carter, A. C.; Bouldin, C. E.; Kenner, K. M.; Bell, M. I.; Woicik, J. C.; Majetich, S. A *Phys. Rev. B.* **1997**, *55*, 13822−13828.
(26) Hamad, K. S.; Roth, R.; Rockenberger, J.; Van Buuren, T.; Alivisatos, A. P. *Phys. Rev. Lett.* **1999**, *83*, 3474−3477.
(27) Scolan, E.; Magnenet, C.; Massiot, D.; Sanchez, C. *J. Mater. Chem.* **1999**, *10*, 2467−2474.
(28) Ladizhansky, V.; Hodes, G.; Vega, S. *J. Phys. Chem. B* **1998**, *102*, 8505−8509.
(29) Elbaum, R.; Vega, S.; Hodes, G. *Chem. Mater.* **2001**, *13*, 2272−2280.
(30) Ladizhansky, V.; Vega, S. *J. Phys. Chem. B* **2000**, *104*, 5237−5241.
(31) Mikulec, F. V.; Kuno, M.; Bennati, M.; Hall, D. A.; Griffin, R. G.; Bawendi, M. G. *J. Am. Chem. Soc.* **2000**, *122*, 2532−2540.
(32) Christiansen, S. C.; Zhao, D.; Janicke, M. T.; Landry, C. C.; Stucky, G.; Chmelka, B. F. *J. Am. Chem. Soc.* **2001**, *123*, 4519−4529.
(33) Thayer, A. M.; Steigerwald, M. L.; Duncan, T. M.; Douglass, D. C. *Phys. Rev. Lett.* **1988**, *60*, 2673−2676.
(34) Sachleben, J. R.; Colvin, V.; Emsley, L.; Wooten, E. W.; Alivisatos, A. P. *J. Phys. Chem. B* **1998**, *102*, 10117−10128.
(35) Sachleben, J. R.; Wooten, E. W.; Emsley, L.; Pines, A.; Colvin, V.; Alivisatos, A. P. *Chem. Phys. Lett.* **1992**, *198*, 431−436.
(36) Cumberland, S. L.; Hanif, K. A.; Khitrov, G. A.; Javier, A.; Strouse, G. F.; Woessner, S. M.; Yun, C. S. *Chem. Mater.* **2002**, *14*, 1576−1584.

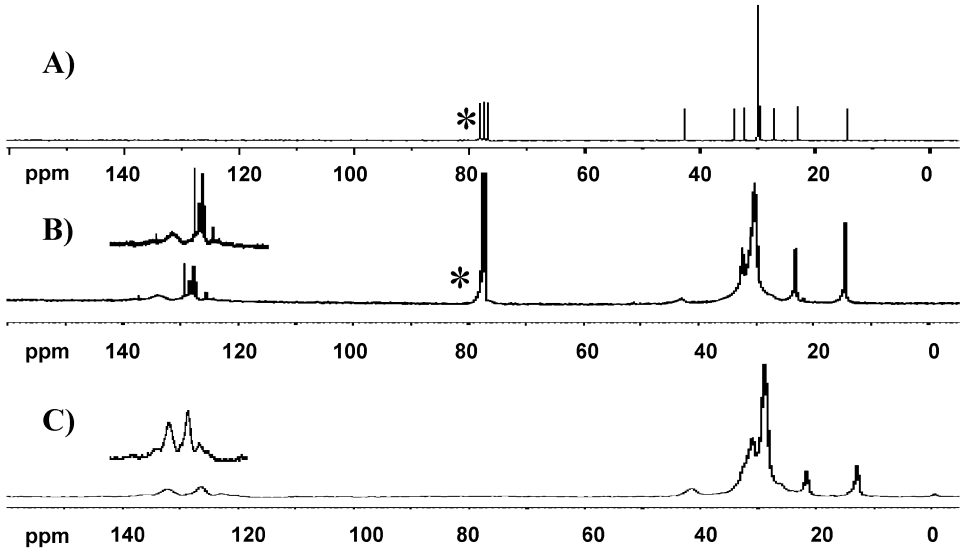

Figure 2. (A) Solution ^{13}C spectra of HDA in $CDCl_3$*. (B) Solution ^{13}C spectra of 2-nm CdSe-HDA in $CDCl_3$*. This spectra shows HDA on the surface of the particle as well as bound and unbound thiophenol. (C) Solid-state ^{13}C MAS of 2-nm CdSe-HDA shows the presence of HDA and thiophenol. The α-carbon of HDA is more pronounced than in solution and is at the same chemical shift as free HDA. (Spinning speed, 12 kHz).

The ^{113}Cd spin−echo experiment was performed with an acquisition time of 2.1 ms, a recycling delay of 120 s, and a 90° and 180° pulse length of 4.5 μs and 9 μs, respectively. The ^{77}Se spin−echo experiment was performed with an acquisition time of 1.6 ms, a recycling delay of 30 s, and a 90° and 180° pulse length of 5.6 μs and 11.2 μs, respectively.

The ^{113}Cd and ^{77}Se CPMAS experiments were acquired using TPPM ^1H decoupling, ramp cross-polarization (CP), an acquisition time of 2.1 ms, a recycling delay of 3 s, contact time ranging from 1 to 25 ms, and a ^1H 90° pulse length of 3 μs.

The 2D $^{13}C\{^1H\}$ HETCOR experiment was performed with a frequency-switched Lee−Goldberg (FSLG) irradiation of 85 kHz applied to the ^1H spins during the t_1 evolution period, ramp CP during mixing with a contact time of 6 ms, a TPPM ^1H decoupling during the data acquisition of 20.6 ms, 1280 scans for each t_1 point for a total of 256 t_1 points, a dwell time of 20 μs, a recycling delay of 1 s, and a ^1H 90° pulse length of 3 μs.

The 2D $^{113}Cd\{^1H\}$ HETCOR and 2D $^{77}Se\{^1H\}$ HETCOR experiments were acquired using ramp CP, TPPM ^1H decoupling, 14 400 scans for each t_1 point for a total of 64 t_1 points, an acquisition time of 1.1 ms, a dwell time of 2 μs, a recycling delay of 1 s, a contact time of 12 ms, and a ^1H 90° pulse length of 3 μs.

Results and Discussion

Surface Passivation. Nanocrystals, which are often modeled using a "spherical" approximation, are crystalline and faceted. The exposed atoms on the facets dictate the nature of the organic passivant interaction and can lead to surface reconstruction following passivant binding. The binding site (chemical shift) and freedom of rotation (line width) of the passivant layer can be probed using solution and solid-state ^{13}C and ^1H NMR in analogy to Pan et al.[37] ^{13}C NMR measurements on HDA-passivated 2-nm CdSe in solution and the solid state are shown in Figure 2. The α-, β-, and γ-carbons in free HDA appear at chemical shifts of 42.5, 34.3, and 27.0 ppm, respectively (Figure 2A). The solution ^{13}C NMR of CdSe-HDA (Figure 2B), shows a broadened α-carbon at the identical chemical shift position as free HDA. The β- and γ-carbons are broadened and poorly resolved because of overlapping peaks with the methylene carbons between 29 and 32 ppm. The observation of an unshifted α-carbon is in contrast to previously published work on alkanethiols[38] on the surface of CdSe nanocrystals, where the chemical shift of the α-carbon is shifted downfield by approximately 5 ppm from that of free ligand. This is not surprising because of the differences in π-back-bonding for a thiol versus an amine ligand and the expected weaker interaction with the surface for alkylamines relative to the thiol passivant.

In addition to the HDA resonances, two broad peaks at 127.2 and 132.9 ppm (Figure 2B) are observed, which can be assigned to carbons of thiophenol bound to the surface of the particle. The narrow peaks between 127 and 129 ppm represent a small amount of free thiophenol in solution and are indicative of thiophenol being in slow exchange on the NMR time scale. In the solid-state, the α-carbon of bound thiophenol (Figure 2C) can be more clearly distinguished than in solution NMR and appears at ∼135 ppm, while the α-carbon of free thiophenol appears at 130.7 ppm, consistent with the expected shift for an α-carbon on a thiol binding to a CdSe surface. The presence of thiophenol on the surface was surprising because of the molar ratio of ∼30:1 HDA/thiophenol for a typical reaction. However, it is known that thiols are better back-bonding ligands than amines, which suggests that either the thiophenol is a better ligator for CdSe or that thiophenol occupies a unique site stabilized under the reaction conditions. The possibility of a unique site for thiophenol is explored by correlation methods below.

The broadening of the carbon peaks for thiophenol, as well as α-, β-, and γ-carbons on HDA in solution NMR (Figure 2B), can be attributed to chemical shift distribution and a decreased T_2 relaxation time due to a lack of rotation upon binding to the CdSe surface.[37−39] Chemical shift distribution was concluded as a likely factor in the broadening of the peaks due to the asymmetry of the line shape of the broadened peaks, although

(37) Pan, C.; Pelzer, K.; Philippot, K.; Chaudret, B.; Dassenoy, F.; Lecante, P.; Casanove, M. *J. Am. Chem. Soc.* **2001**, *123*, 7584−7593.

(38) Cumberland, S. L.; Berrettini, M. G.; Javier, A.; Strouse, G. F. *Chem. Mater.* **2003**, *15*, 1047−1056.

(39) Badia, A.; Gao, W.; Singh, S.; Demers, L.; Cuccia, L.; Reven, L. *Langmuir* **1996**, *12*, 1262−1269.

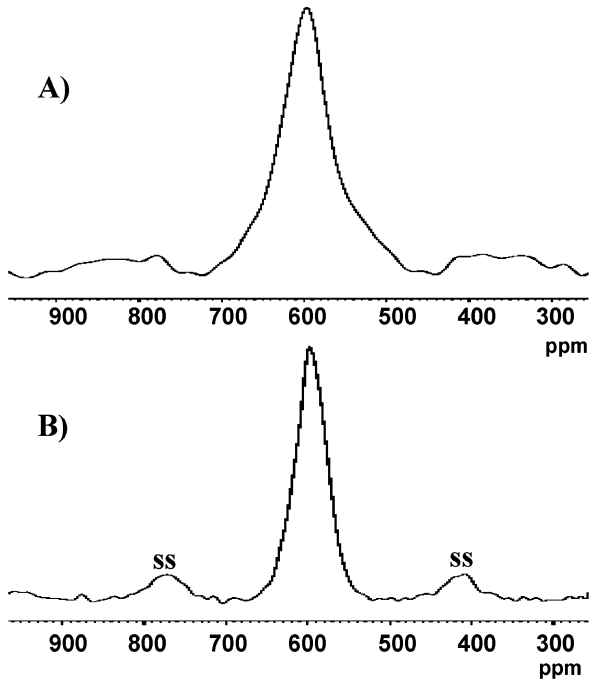

Figure 3. (A) ^{113}Cd spin−echo spectra of 2-nm CdSe-HDA measures all the cadmium in the particle. (B) ^{1}H−^{113}Cd CPMAS spectra of 2-nm CdSe-HDA (15 ms contact time) measures the surface or near-surface cadmium in the particle. (Spinning speed in A and B, 12 kHz.)

chemical shift anisotropy was concluded to be improbable because of identical line shapes of the broadened peaks in the solution and solid-state NMR spectra. As seen in Figure 2C, the carbons of thiophenol and the α-carbon of HDA become more pronounced in the solid-state than in solution NMR because of external averaging by MAS the dipolar interactions from the decreased rotation. In the MAS spectra, the β- and γ-carbons of HDA are unresolved because of instrumental resolution limits giving rise to an overlap with the methylene chain carbons. As can be seen by comparison of the line widths for the carbon atoms in solution and solid-state NMR of CdSe-HDA, the rotation in the chain increases as you move down the chain toward the methyl group, as evidenced by the observation of narrowing lines. Carbon 15 and the methyl carbon at 22.9 and 14.2 ppm, respectively, are similar to the line width of free HDA, indicating that the terminal carbons do not experience hindered rotation and therefore are likely rotationally disordered with respect to the surface of the nanomaterial. A loss of signal intensity and a broadening for the α-, β-, and γ-^{13}C peaks, which are closest to the NC surface, when compared to C_{15} is predicted for these materials because of rotational constraints for the passivants on the nanomaterial surface, as previously observed by FT-IR measurements of packing motifs on CdSe surfaces.[21,22] Amorphous packing would tend to lead to a shift in the NMR position also, but only a small change in the line widths for the α-, β-, and γ-carbons because of the increased rotational freedom of amorphously structured surfaces.

Cadmium and Selenium Surface Structure. Knowledge of the site homogeneity of cadmium and selenium on the surface and in the core of the particle can be gained by ^{113}Cd and ^{77}Se NMR experiments, including spin−echo and CPMAS. In Figure 3A, the ^{113}Cd spin−echo experiment for CdSe-HDA measures all of the ^{113}Cd in the nanocrystal (core and surface) and was chosen because of its pulse sequence ($\pi/2-\tau-\pi-\tau-$acquisition) being useful for materials with broad NMR peaks. The pulse sequence minimizes problems due to *rf* bleeding and receiver recovery. The ^{1}H−^{113}Cd CPMAS experiment was conducted with contact times between 1 and 25 ms; a typical CPMAS spectra for 15 ms contact time is shown in Figure 3B. CPMAS measures only cadmium atoms at or near the surface of the particle because of polarization transfer from the abundant ^{1}H spins on the ligands to the ^{113}Cd spins via nuclear dipole−dipole interaction,[28,29] which follows a $1/R^3$ distance dependence (normally ∼5 Å maximum). The peak shape and chemical shift is consistent throughout the various mixing times, while only the intensity changes because of building up of the signal with increasing mixing time, followed by a decrease through ^{1}H $T_{1\rho}$ relaxation.[40−42]

The main peak in both the spin−echo experiment and the CPMAS experiment is centered at 595 ppm, which is very near the bulk hexagonal CdSe value of 585 ppm (Supporting Information Figure 1A), suggesting a low level of reconstruction of cadmium in the particle or an insensitivity of cadmium to its chemical environment. Because of the chemical shift range of only 87 ppm between bulk and the precursor, $[Li]_4[Cd_{10}Se_4(SC_6H_5)_{16}]$ (Supporting Information Figure 1B), we believe the latter to be most likely, which limits the usefulness of ^{113}Cd NMR for analysis of the reconstruction of cadmium sites. The broad feature of the ^{113}Cd spectra indicate chemical shift distribution and fast relaxation of cadmium atoms in the solid state. The spin−echo peak is broader than the CPMAS peak, which arises from the larger distribution of chemical sites in the total particle (core and surface) relative to just the Cd sites on or near the surface probed by CPMAS spectra.[31]

The selenium NMR of the total Se atoms in the nanoparticle (spin−echo) and the Se atoms on or near the surface (CPMAS) for 2-nm CdSe-HDA are shown in Figure 4, with a line width and population analysis generated from a least-squares fit of the data in Table 1. Considering the error arising from a combination of instrumental and statistical contributions, the predicted error on the Se site shifts, line widths, and percentages are ±2 ppm, ±100 Hz, and ±3%, respectively. This includes contributions from signal-to-noise and deconvolution of peaks. The percentage site occupancy error is determined by standard deviation analysis of data from all mixing times measured. The population is corrected for the ^{1}H−^{77}Se cross-relaxation time constants, T_{SeH}, which are shown in Table 2. To our knowledge, these are the first solid-state ^{77}Se NMR experiments on lyothermally prepared CdSe nanocrystals reported in the literature. In contrast to ^{113}Cd NMR, the ^{77}Se spin−echo spectrum (Figure 4A) reveals a series of selenium sites at various chemical shifts with contributions from both the core and surface selenium atoms. This is not surprising since the sensitivity of the ^{77}Se to the chemical environment is more significant, as seen by a larger chemical shift range of 275 ppm between selenium in bulk CdSe and selenium in the precursor (Supporting Information Figure 2). The center of the largest peak in the spin−echo spectrum is at −635 ppm (Figure 4A) and correlates with the largest peak observed in the ^{1}H−^{77}Se CPMAS (Figure 4B) spectra. This

(40) Gabrielse, W.; Gaur, A. G.; Feyen, F. C.; Veeman, W. S. *Macromolecules* **1994**, *27*, 5811−5820.
(41) Voelkel, R. *Angew. Chem., Int. Ed. Engl.* **1988**, *27*, 1468−1483.
(42) Klein Douwel, C. H.; Maas, W. E. J. R.; Veeman, W. S.; Werumeus Buning, G. H.; Vankan, J. M. J. *Macromolecules* **1990**, *23*, 406−412.

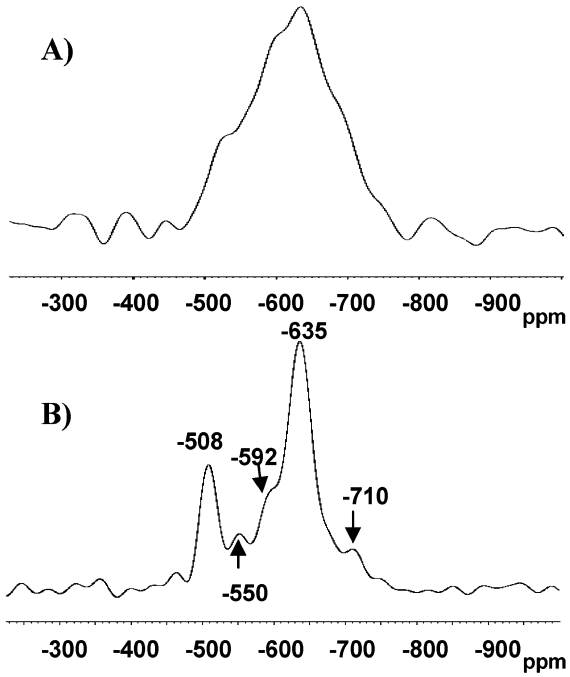

Figure 4. (A) ^{77}Se spin−echo spectra of 2-nm CdSe-HDA measures all of the selenium in the particle. (B) ^{1}H−^{77}Se CPMAS spectra of 2-nm CdSe-HDA (15 ms contact time) measures the surface or near-surface selenium in the particle. (Spinning speed in A and B, 12 kHz.)

Table 1. Analysis of the CPMAS ^{77}Se Sites Frequency, Line Width, and Population Using a Linear Least Squares Fit of the Data at 15 ms Mixing Time[a]

Se site (PPM)	line width (Hz)	percentage
−508	1688	16
−550	1860	10
−592	1997	14
−635	2232	55
−676[b]	*1803*	<5
−710[b]	*1946*	<5

[a] The population is corrected for the ^{1}H−^{77}Se cross-relaxation time constant T_{SeH}. [b] The shoulder at −676 ppm and the less intense peak at −710 ppm are included in the deconvolution of the total spectra. However, because of the magnitude of error in measurement of this peak and estimation of T_{SeH}, no attempt to assign a percentage to the peak has been made.

suggests that the signal arises from selenium at or near the surface of the 2-nm particle, with the spin−echo signature reflecting the ∼48% of the particle being attributable to surface atoms relative to the core atoms in this size regime.[43]

The presence of five narrow ^{77}Se peaks being observed in the ^{1}H−^{77}Se CPMAS spectra (Figure 4B), at −508, −550, −592, −635, and −710 ppm is surprising. This observation suggests that the surfaces of the 2-nm particles represent reconstructed sites that remain largely ordered in the structure rather than forming an amorphous ensemble structure. If the nanomaterials were amorphous, a single broad peak would have been expected. Repeating this experiment while varying the contact time, τ, between 1 and 25 ms, indicates no new features

(43) The value of 46−50% surface atoms, defined as the ratio of atoms with dangling bonds to those with 4-fold coordination, was determined from analyzing several near-spherical, faceted ∼2-nm CdSe wurtzite crystals (170−195 atoms) created in Crystal Impact's Diamond software, with singly bound atoms removed. C_{3v} point group symmetry and the lattice parameters $a = 4.3$A, $c = 7.0$A were used for this estimate.

Table 2. 2-nm CdSe-HDA ^{77}Se Cross-Relaxation Time Constants, T_{SeH}, (milliseconds)

^{77}Se peak (ppm)	T_{SeH} (ms)
−508	13.5 ± 0.5
−550	8.0 ± 0.5
−592	5.9 ± 0.5
−635	6.4 ± 0.5

and only intensity changes due to building up of the signal with increasing contact time followed by a decrease due to $T_{1\rho}$ relaxation.

The nature and position of the five sites can be investigated by the ^{1}H−^{77}Se cross-relaxation time constants, T_{SeH}. The integrated ^{77}Se peak intensities from ^{1}H−^{77}Se CPMAS were plotted as a function of the contact time, τ. The proton spin−lattice time constant, $T_{1\rho}$, was determined following a procedure from a previous publication.[41] The plot was fit to eq 1[44] using nonlinear least-squares analysis to determine T_{SeH}. The fitted plots can be viewed in Supporting Information Figure 3.

$$M(\tau) = M_0(\exp(-\tau/T_{1\rho H}) - \exp(-\tau/T_{SeH}))/(1 - T_{SeH}/T_{1\rho H}) \quad (1)$$

The magnitude of T_{SeH} is dependent on the intermolecular distance between ^{1}H and ^{77}Se centers. Assuming that the surface seleniums have similar mobility, the cross-relaxation time constant has a $1/R^6$ distance dependence and can be used to compare distances.[42] The values of T_{SeH} for four out of the five sites of selenium are summarized in Table 2. The plot of intensity versus contact time for the ^{77}Se peak at −710 ppm was not fit because of the poor signal-to-noise ratio. The peaks at −550, −592, and −635 ppm all have similar cross-relaxation time constants, with T_{SeH} values of 8.0, 5.9, and 6.4 ms (Table 2), respectively, indicating similar average distances between these Se sites and the ligand protons. In addition, these Se sites are closer to ligand protons than the Se sites at −508 ppm, as reflected by the larger T_{SeH} value (13.5 ms) of the latter. This is consistent with the assignment of −508 ppm as an internal Se site (one layer down). With this information, we conclude that the peaks at −550, −592, and −635 ppm all represent surface sites. If we approximate the intensity of the peaks as a measure of the number of seleniums in each site (Table 1), which is reasonable based on the similar value for T_{SeH} for these sites, then the series of peaks from −550 to −635 ppm would represent increasing selenium occupation in each site. Considering the site occupation and available types of sites on a 2-nm CdSe, we believe that the sites at −550, −592, and −635 ppm represent selenium occupying a vertex, edge, and facet site on the nanoparticle, respectively. The chemical shift decrease from vertex to facet site also supports the assignment because of a facet site most likely being more shielded from increased ligand density than a vertex or edge; using the same argument, an edge site will be more shielded than a vertex. From the chemical shift of the peak at −710 ppm, a likely assignment for this peak would be a facet site reconstructed differently than the peak at −635 ppm. Taking into account that the peak at −508 ppm is at a longer distance from the ligand protons and that its chemical shift is closest to the bulk ^{77}Se value of −474 ppm (Supporting Information Figure 2B), we conclude that the −508 ppm site arises from the tetrahedrally coordinated selenium site one layer

(44) Mehring, M. *High-Resolution NMR Spectroscopy in Solids*; Springer-Verlag: New York, 1976.

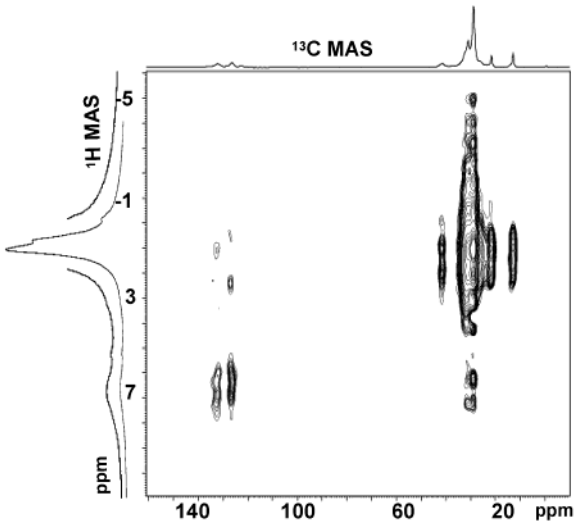

Figure 5. 2D $^{13}C\{^1H\}$ HETCOR NMR of 2-nm CdSe-HDA. Separate single pulse ^1H MAS (traditional and magnified view) and ^{13}C MAS spectra reside along the vertical and horizontal axes of the contour plot, respectively. The correlation between thiophenol and HDA indicates that thiophenol is interacting with the middle of the HDA chain. (Spinning speed, 12 kHz; contact time, 6 ms.)

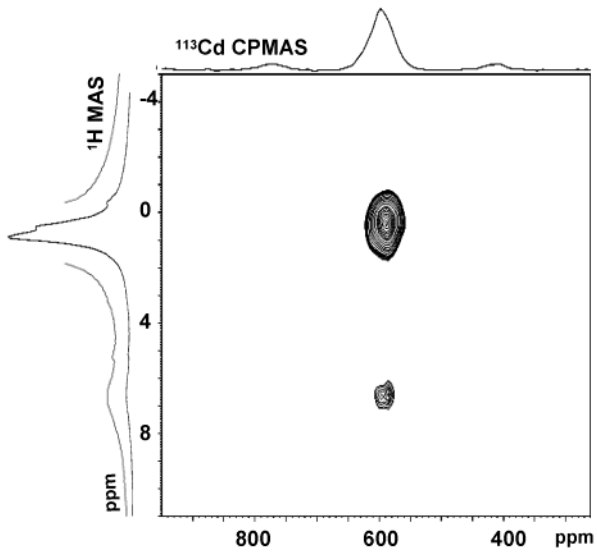

Figure 6. 2D $^{113}C\{^1H\}$ HETCOR NMR of 2-nm CdSe-HDA. Separate single pulse ^1H MAS and $^1H-^{113}Cd$ CPMAS spectra reside along the vertical and horizontal axes of the contour plot, respectively. The HETCOR correlations show that the surface cadmium are interacting strongly with the HDA methylene chain protons and with the protons of thiophenol, consistent with HDA and thiophenol bound to cadmium on the surface of the particle. (Spinning speed, 12 kHz; contact time, 12 ms.)

down from the surface. The observation of shift in the NMR signatures for the selenium sites from bulk supports particle reconstruction both at the surface and within the 2-nm CdSe nanoparticle.

Thiophenol vs HDA Site Occupation. The occurrence of both thiophenol and HDA in the 2-nm CdSe dot does raise the question of site selectivity for binding on the CdSe facet. Using correlated NMR methods, we obtained the passivant site occupation by investigating the 2D HETCOR NMR experiments. The $^{13}C\{^1H\}$ frequency-switched Lee−Goldberg (FSLG) HETCOR experiment is shown in Figure 5, with separately measured single pulse ^1H MAS on the vertical axis in a traditional and magnified view and ^{13}C MAS spectra on the horizontal axis. The protons on the HDA chain appear between −0.8 and 1.8 ppm, and the protons on thiophenol appear between ∼5.8 and 7.4 ppm, as seen from the correlations with their respective carbons in Figure 5. The amine protons are not seen because of broadening to the baseline from lack of rotation. FSLG HETCOR, which significantly increases homonuclear decoupling in the ^1H dimension, was chosen for this experiment to increase resolution to clearly distinguish the region of the HDA chain that is interacting with thiophenol by the correlations of thiophenol to HDA and to eliminate the ^1H spin diffusion mechanism.

As seen in Figure 5, the correlation from thiophenol protons at 6.8 ppm in the ^1H dimension to the carbons of HDA at approximately 30 ppm in the ^{13}C dimension indicates that thiophenol is strongly interacting with the middle of the HDA chain. This information establishes that thiophenol is in close proximity to the middle of the HDA chain. On the basis of this observation, it appears the ligands are residing on the same face rather than face selective capping of the two species, which would presumably give no correlation. There is the possibility if the ligands were on neighboring faces and with the proper tilt angles that there could be an interaction with the middle of the chain, but this would only be at the intersections leading to the observation of a weak correlation.

The $^{113}Cd\{^1H\}$ HETCOR experiment is shown in Figure 6, with separately measured single pulse ^1H MAS in a traditional and magnified view and $^1H-^{113}Cd$ CPMAS spectra on the vertical and horizontal axes, respectively. There is a correlation of the ^1H region of HDA between approximately −0.8 to 1.8 ppm, with the surface cadmium centered at 595 ppm. There is also a correlation with the thiophenol protons centered at 6.79 ppm to this cadmium peak. This information provides direct proof that the protons on HDA and thiophenol are strongly interacting with the surface cadmium, which is consistent with both ligands being bound to cadmiums on the surface of the particle.

The $^{77}Se\{^1H\}$ HETCOR experiment is shown in Figure 7, with separately measured single pulse ^1H MAS on the vertical axis in a traditional and magnified view and $^1H-^{77}Se$ CPMAS spectra on the horizontal axis, respectively. There are five correlation peaks between the methylene chain of HDA and the five selenium sites. An amine−selenium bond is unlikely; therefore, we have concluded that these correlations signify that the methylene protons of HDA strongly interact with the selenium sites, arising from a chain tilt of HDA on nearby cadmium atoms toward the surface. This type of configuration would allow the chain to be in a close proximity to selenium as shown in Figure 8A, consistent with previous work on CdSe that indicated a maximum chain tilt toward the surface at small nanocrystal sizes.[22] Unfortunately, because of the length of time for this experiment (504 h), it was not possible to repeat the experimental measurements at various mixing times; however, we believe spin diffusion is not a significant contribution to the observation because of the high spinning speed, different $T_{1\rho}$ values for protons on the HDA chain, and that FSLG homonuclear ^1H decoupling does not significantly improve ^1H resolution in the indirect dimension in ^{13}C and ^{113}Cd HETCOR NMR. There are no correlations between the selenium sites and thiophenol, which indicates that the thiophenol protons are not in close proximity to selenium, and more importantly, the five

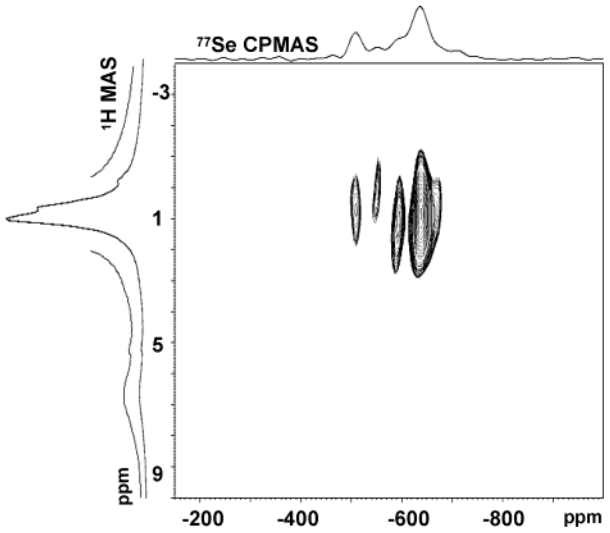

Figure 7. 2D $^{77}Se\{^{1}H\}$ HETCOR NMR of 2-nm CdSe-HDA. Separate single pulse ^{1}H MAS and $^{1}H-^{77}Se$ CPMAS spectra reside along the vertical and horizontal axes of the contour plot, respectively. The HETCOR correlations determine that the five separate Se sites are interacting strongly with the HDA methylene chain protons consistent with a chain tilt of HDA to the surface. (Spinning speed, 12 kHz; contact time, 12 ms.)

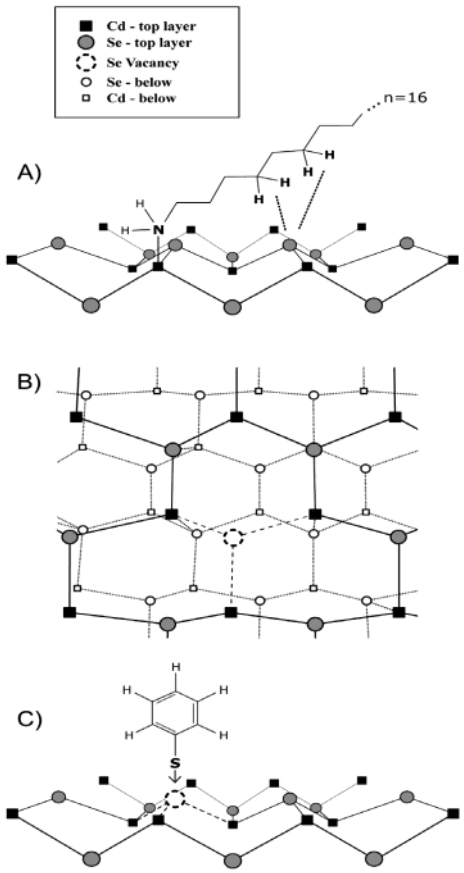

Figure 8. (A) Chain tilt of HDA to the surface of the particle. (B) Selenium vacancy on the surface of a CdSe nanocrystal. (C) A thiophenol molecule filling a selenium vacancy.

observed selenium sites in the 2-nm CdSe nanocrystal do not arise from thiophenol binding.

Structural Model. The combined experimental results lead to a structural model for the surface of a 2-nm CdSe as shown in Figure 8. The exact site of thiophenol on the CdSe nanocrystal

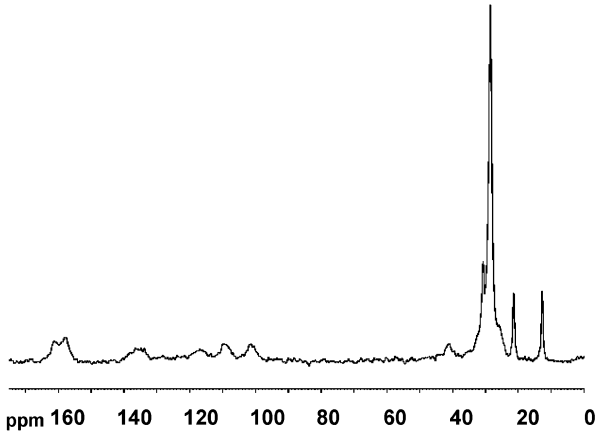

Figure 9. Solid-state ^{13}C MAS of 2-nm CdSe-HDA in which the thiophenol has been ligand exchanged with 2,4-difluorothiophenol.

is not known; however, it appears to sit on a special site, potentially a cadmium surface reconstruction site (Figure 8C). Evidence for this positional assignment arises from data obtained by ^{13}C MAS of 2-nm CdSe-HDA that has been ligand-exchanged with 2,4-difluorothiophenol (Figure 9). Following ligand exchange with 2,4-difluorothiophenol, HDA is still present but thiophenol has been completely replaced. The peaks at 159 and 162 ppm represent the 2 and 4 carbons with attached fluorines, respectively. Carbons 1, 3, 5, and 6 appear at 138, 102, 110, and 118 ppm, respectively. To our surprise, adding a fluorinated-thiophenol derivative to the material, followed by the usual ligand exchange protocol, does not displace the HDA as a strong binding ligand would be expected to do; instead, the fluorinated thiophenol only displaces bound thiophenol as evidenced by recapping with 2,4-difluorothiophenol (Figure 9). Another interesting fact pointing to the assignment of a special site for a thiophenol is the observation that we could not displace thiophenol with HDA or pyridine by usual ligand exchange protocols.

The combination of these results and the information that the thiophenol protons are not in close proximity to any of the selenium sites from the $^{77}Se\{^{1}H\}$ HETCOR experiment strongly suggests a unique cadmium site occupation. We believe a likely model would be thiophenol filling selenium vacancies (Figure 8B,C) on the surface of the particle. In this configuration, the protons on thiophenol would not be in close proximity to selenium on the surface of the particle as seen in the $^{77}Se\{^{1}H\}$ HETCOR experiment (Figure 7). This type of interaction also supports the presence of thiophenol from the reaction and the recapping results. This theory of vacancy filling seems very plausible, but more experiments need to be carried out to fully analyze this model.

Conclusion

A model of the surfaces and interfaces of 2-nm CdSe nanocrystals synthesized from a single source precursor method has been constructed by solution and solid-state NMR experiments. This model includes the presence of thiophenol and HDA ligands on the surface of the particle characterized by solution and solid-state ^{13}C NMR. It was established through $^{113}Cd\{^{1}H\}$ HETCOR NMR that these ligands are bound to the surface through bonds to surface cadmium atoms. ^{77}Se CPMAS NMR indicates five sites for selenium, which can be correlated to facet,

edge, or vertex sites and to selenium a layer deep. This technique also suggests a largely crystalline surface with selenium site reconstruction. $^{77}Se\{^{1}H\}$ HETCOR NMR establishes the close proximity of selenium to the HDA chain, which supports a chain tilt of the HDA to the surface of the particle. This experiment also establishes that thiophenol is not in close proximity to the five selenium sites. The combination of these results and various ligand exchange results suggest that thiophenol is filling selenium vacancies on the surface. More experiments are in progress for a size-dependent study of this material and also to investigate this vacancy-filling theory.

Acknowledgment. This work was supported in part by the National Science Foundation Career Grant (G.F.S.). We thank Professor Brad Chmelka for valuable discussions on crystallinity and cross-polarization.

Supporting Information Available: ^{113}Cd and ^{77}Se CPMAS NMR of the precursor, $Li_4[Se_4Cd_{10}(SPH)_{16}$, as well as ^{113}Cd and ^{77}Se spin−echo NMR of bulk wurtzite CdSe and the integrated ^{77}Se peak intensities from $^{1}H-^{77}Se$ CPMAS (PDF). This material is available free of charge via the Internet at http://pubs.acs.org.

JA037228H